Electronic supplementary information

A carbon-functionality-appended diborylacetylene available for a component of organic synthesis and OLEDs

Tetsuyoshi Tsukada, Yoshiaki Shoji,* Kumiko Takenouchi, Hideo Taka and Takanori Fukushima*

*To whom correspondence should be addressed.
E-mail: yshoji@res.titech.ac.jp (Y.S.); fukushima@res.titech.ac.jp (T.F.)

Table of Contents

1. Materials and methods

Handling of air- and/or moisture-sensitive compounds were performed either using standard Schlenk-line techniques or in a glove box under argon. Column chromatography was carried out using Silica Gel 60 N (spherical, neutral, particle size: 63–210 mm, Kanto Chemical Co., Inc.). Anhydrous CH_2Cl_2, hexane, toluene and tetrahydrofuran (THF) were dried by passage through an activated alumina column and a Q-5 column (Nikko Hansen & Co., Ltd.). Deuterated chloroform ($CDCl_3$) was dried over CaH_2 and freshly distilled prior to use. 10-Bromo-9-oxa-10-boraanthracene[S1] (**2$_H$**) and 4,4'-di-*tert*-butyldiphenyl ether[S2] were prepared according to reported procedures.

Fourier transform infrared (FT-IR) spectra were recorded at 25℃ with a JASCO model FT/IR-6600 Fourier transform infrared spectrometer. Nuclear magnetic resonance (NMR) spectroscopy measurements were carried out on a Bruker model AVANCE-400 spectrometer (400.0 MHz for ^{1}H) or on a Bruker model AVANCE III HD-500 spectrometer (^{1}H: 500.0 MHz, ^{11}B: 160.4 MHz, ^{13}C: 125.7 MHz), where are expressed relative to the resonances of the residual non-deuterated solvent for ^{1}H ($CDCl_3$: ^{1}H(δ) = 7.26 ppm), external $BF_3{\cdot}Et_2O$ in $CDCl_3$ for ^{11}B (^{11}B(δ) = 0.0 ppm), and the resonances of the residual solvent for ^{13}C ($CDCl_3$: ^{13}C(δ) = 77.16 ppm). The absolute values of the coupling constants are given in Hertz (Hz), regardless of their signs. Multiplicities are abbreviated as singlet (s), doublet (d), triplet (t), multiplet (m) and broad (br). Mass spectrometry measurements were carried out on a Bruker micrOTOF II mass spectrometer equipped with an atmospheric pressure chemical ionization (APCI) probe. Electronic absorption spectra were recorded using a quartz cell on a JASCO model V-670 UV/VIS spectrophotometer. Fluorescence and phosphorescence spectra as well as phosphorescence lifetime were measured using a quartz cell or KBr plates on a JASCO model FP-8500 spectrophotometer. The absolute PLQY values were measured by a Hamamatsu Phåotonics model Quantaurus-QYC11347 absolute PLQY spectrometer. Cyclic voltammetry measurements were conducted using an ALS Instruments model 622C electrochemical analyzer (working and counter electrodes: Pt wire; pseudo-reference electrode: Ag wire). Thermogravimetric analysis (TGA) was performed on a SHIMADZU TGA-50 analyzer.

2. Synthesis

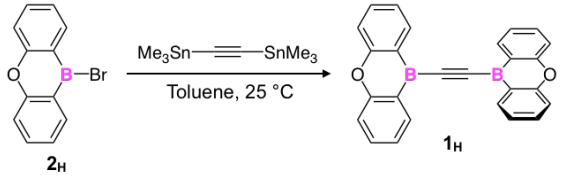

Compound 1$_H$. Under argon, a toluene solution (6 mL) of bis(trimethylstannyl)acetylene (784 mg, 2.23 mmol) was added dropwise to a toluene solution (6 mL) of 10-bromo-9-oxa-10-boraanthracene (592 mg, 2.23 mmol) at 25 °C, and the resulting mixture was stirred at 25 °C for 1 h. The pale-yellow precipitate formed in the reaction mixture was collected by filtration, washed with hexane (5 mL x 3), and dried under reduced pressure to give **1$_H$** as a pale-yellow powder (402 mg, 1.05 mmol) in 92% yield: FT-IR (ATR): ν (cm^{-1}) 3853, 3840, 3736, 3649, 3566, 2939, 2871, 2372, 2362, 2355, 2335, 1604, 1575,

1542, 1507, 1473, 1434, 1332, 1313, 1261, 1153, 1097, 1058, 911, 756, 642. ^{1}H NMR (500 MHz, $CDCl_3$, 25 °C): δ (ppm) 8.44 (dd, J = 7.7, 1.6 Hz, 4H), 7.77 (ddd, J = 8.5, 7.0, 1.6 Hz, 4H), 7.61 (dd, J = 8.5, 0.9 Hz, 4H), 7.38 (ddd, J = 7.7, 7.0, 0.9 Hz, 4H). ^{11}B NMR (160 MHz, $CDCl_3$, 25 °C): δ (ppm) 43.7 (br). ^{13}C NMR (125 MHz, $CDCl_3$, 25 °C): δ (ppm) 159.9, 136.5, 135.2, 122.8, 117.7, two peaks of the carbon atoms (*ipso*-positions to the boron atoms) were not observed. APCI-TOF mass: calcd for $C_{26}H_{16}B_2O_2$ $[M]^+$: m/z=382.1340; found: 382.1310. ^{1}H, ^{11}B and ^{13}C NMR spectra of $\mathbf{1_H}$ are shown in Figs. S9, S10 and S11, respectively.

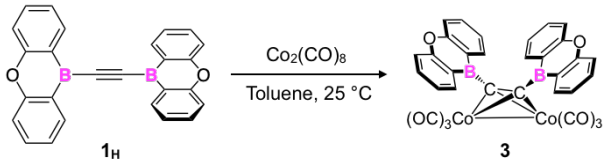

$\mathbf{1_H}$ **3**

Cobalt complex 3. Under argon, a toluene solution (5 mL) of $Co_2(CO)_8$ (185 mg, 0.541 mmol) was added dropwise to a toluene solution (5 mL) of $\mathbf{1_H}$ (200 mg, 0.524 mmol), and the resulting mixture was stirred at 25 °C for 4 h and then evaporated to dryness under reduced pressure. The residue was recrystallized from toluene to give **3** as a dark-green crystalline material (257 mg, 0.385 mmol) in 73% yield: FT-IR (ATR): ν (cm^{-1}) 3076, 2086, 2046, 2019, 1999, 1867, 1737, 1598, 1575, 1508, 1473, 1448, 1431, 1331, 1306, 1245, 1202, 1154, 1128, 1057, 1032, 907, 755, 736, 707, 659, 612, 586, 571, 546, 523, 517, 508. ^{1}H NMR (500 MHz, $CDCl_3$, 25 °C): δ (ppm) 8.36 (d, J = 7.5 Hz, 4H), 7.69 (dd, J = 8.4, 7.5 Hz, 4H), 7.58 (d, J = 8.4 Hz, 4H), 7.19 (dd, J = 8.4, 7.5 Hz, 4H). ^{11}B NMR (160 MHz, $CDCl_3$, 25 °C): δ (ppm) 45.5 (br). ^{13}C NMR (125 MHz, $CDCl_3$, 25 °C): δ (ppm) 200.0, 159.7, 134.3, 133.5, 122.4, 118.1, two peaks of the carbon atoms (*ipso*-positions to the boron atoms) were not observed. ^{1}H, ^{11}B and ^{13}C NMR spectra of **3** are shown in Figs. S12, S13 and S14, respectively.

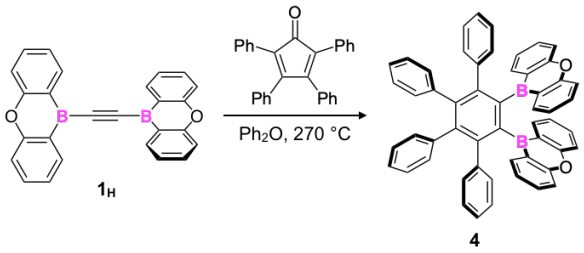

$\mathbf{1_H}$ **4**

Compound 4. Under argon, a diphenylether solution (6 mL) of a mixture of $\mathbf{1_H}$ (400 mg, 1.05 mmol) and tetraphenylcyclopentadienone (403 mg, 1.05 mmol) was heated at 270 °C for 24 h. The reaction mixture was evaporated to dryness under reduced pressure. The residue was subjected to column chromatography (SiO_2, CH_2Cl_2/hexane 2/3 v/v) to allow isolation of **4** as a brown powder (487 mg, 0.659 mmol) in 63% yield: FT-IR (ATR): ν (cm^{-1}) 3464, 3005, 2970, 2950, 2880, 2837, 1576, 1558, 1541, 1507, 1472, 1455, 1422, 1364, 1260, 1227, 1216, 1145, 1116, 1067, 1014, 945, 905, 878, 832, 757, 731, 689, 625, 612, 596, 556, 539, 526, 517, 509, 481. ^{1}H NMR (500 MHz, $CDCl_3$, 25 °C): δ (ppm) 8.35 (dd, J = 7.7. 1.6 Hz, 4H), 7.81 (ddd, J = 8.4, 7.0, 1.6 Hz, 4H), 7.57 (dd, J = 8.4, 1.2 Hz, 4H), 7.40 (ddd, J = 7.7, 7.0, 1.2 Hz, 4H), 7.23–7.25 (m, 12H), 7.16–7.20 (m, 4H), 6.92–6.95 (m, 4H). ^{11}B NMR (160 MHz, $CDCl_3$, 25 °C): δ (ppm) 52.4 (br). ^{13}C NMR (125 MHz, $CDCl_3$, 25 °C): δ (ppm) 159.7, 136.3, 135.0, 134.3, 131.6, 130.4, 130.0, 129.7, 128.6, 126.9, 126.4, 122.7, 122.5, 117.6, 111.6, two peaks of

the carbon atoms (*ipso*-positions to the boron atoms) were not observed. APCI-TOF mass: calcd for $C_{26}H_{16}B_2O_2$ $[M]^+$: *m*/*z*=738.2913; found: 738.3048. ^{1}H, ^{11}B and ^{13}C NMR spectra of **4** are shown in Figs. S15, S16 and S17, respectively.

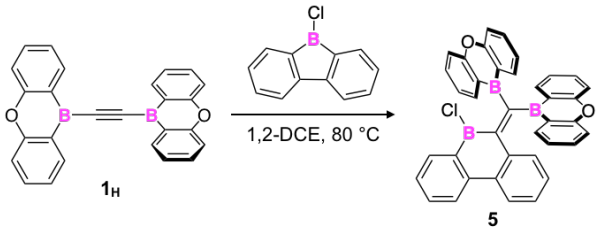

Compound 5. Under argon, a 1,2-dichloroethane solution (4 mL) of a mixture of **1H** (101 mg, 0.265 mmol) and 9-chloro-9-borafluorene (52 mg, 0.261 mmol) was heated at 80 °C for 96 h. The yellow suspension formed in the reaction mixture was collected by filtration, washed with hexane (2 mL x 3) and dried under reduced pressure to give **5** as a yellow powder (103 mg, 0.177 mmol) in 68% yield: FT-IR (ATR): *v* (cm^{-1}) 3016, 2969, 2940, 2882, 2836, 1738, 1600, 1573, 1540, 1507, 1474, 1447, 1428, 1372, 1328, 1302, 1287, 1263, 1216, 1204, 1152, 1132, 1107, 1099, 1029, 967, 910, 843, 793, 753, 727, 709, 686, 657, 610, 593, 566, 550, 529, 517, 510, 497. ^{1}H NMR (500 MHz, $CDCl_3$, 25 °C): δ (ppm) 8.02 (d, J = 2.6, 1H), 8.00 (d, J = 2.0 Hz, 1H), 7.86 (dd, J = 7.9, 1.5 Hz, 2H), 7.72 (dd, J = 7.7, 1.5 Hz, 2H), 7.67 (d, J = 8.0 Hz, 1H), 7.61–7.64 (m, 4H), 7.36–7.44 (m, 5H), 7.26 (td, J = 9.1, 1.7 Hz, 2H), 7.16–7.23 (m, 4H), 7.00 (td, J = 7.7, 1.5 Hz, 2H). ^{11}B NMR (160 MHz, $CDCl_3$, 25 °C): δ (ppm) 57.7 (br), 50.2 (br). ^{13}C NMR (125 MHz, $CDCl_3$, 25 °C): δ (ppm) 152.3, 142.1, 140.4, 133.8, 132.8, 132.6, 132.1, 131.0, 129.8, 129.5, 129.4, 129.2, 128.5, 128.4, 127.1, 124.9, 123.6, 121.9, 116.2, 110.3, 101.2, five peaks of the carbon atoms (*ipso*-positions to the boron atoms) were not observed. APCI-TOF mass: ion peaks assignable to the corresponding hydrolyzed product with a B–OH moiety were observed; calcd for $C_{38}H_{25}B_3O_3$ $[M]^+$: m/z = 562.2095; found: 562.2351. ^{1}H, ^{11}B and ^{13}C NMR spectra of **5** are shown in Figs. S18, S19 and S20, respectively.

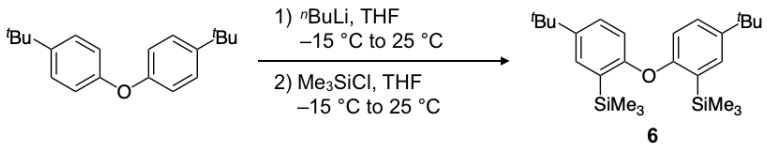

Compound 6. Under argon at –15 °C, *n*-butyllithium (2.6 M hexane solution, 30 mL, 77.5 mmol) was added dropwise over a period of 20 min to a THF solution (120 mL) of 4,4'-di-*tert*-butyldiphenyl ether (7.30 g, 25.9 mmol), and the resulting mixture was stirred at –15 °C for 1 h and then allowed to warm to 25 °C. After being stirred at 25 °C for 18 h, chlorotrimethylsilane (7.3 mL, 56.9 mmol) was added dropwise to the reaction mixture at –15 °C, and the mixture was stirred at –15 °C for 1 h and then allowed to warm to 25 °C. After being stirred at 25 °C for 2 h, the reaction mixture was poured into water and extracted with hexane. A combined organic extract was washed with water and brine, dried over anhydrous Na_2SO_4, and evaporated to dryness under reduced pressure. The residue was subjected to column chromatography (SiO_2, hexane) to allow isolation of **6** as a white powder (1.98 g, 4.64 mmol) in 18% yield: FT-IR (ATR): *v* (cm^{-1}) 3018, 2950, 2897, 2776, 2889, 2791, 1748, 1717, 1653, 1577,

1741, 1497, 1469, 1377, 1360, 1263, 1245, 1214, 1145, 1117, 1077, 1067, 896, 878, 831, 817, 756, 731, 689, 626, 595, 556, 540, 526, 515, 509, 468, 436. ^{1}H NMR (500 MHz, $CDCl_3$, 25 °C): δ (ppm) 7.48 (d, J = 2.5 Hz, 2H), 7.26 (dd, J = 8.6, 2.5 Hz, 2H), 6.60 (d, J = 8.6 Hz, 2H), 1.34 (s, 18H), 0.34 (s, 18H). ^{13}C NMR (125 MHz, $CDCl_3$, 25 °C): δ (ppm) 161.2, 144.7, 131.5, 129.5, 127.7, 118.0, 34.3, 31.6, –0.5. APCI-TOF mass: calcd for $C_{26}H_{42}OSi_2$ $[M]^+$: m/z=426.2769; found: 426.2814. ^{1}H and ^{13}C NMR spectra of **6** are shown in Figs. S21 and S22, respectively.

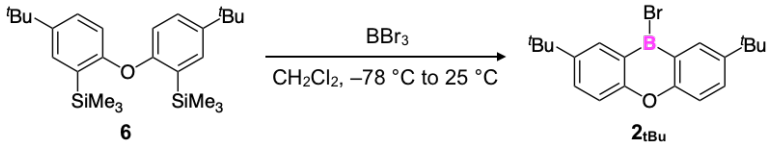

Compound $\mathbf{2_{tBu}}$. Under argon at –78 °C, boron tribromide (0.25 M in dichloromethane, 4.0 mL, 10 mmol) was added dropwise to a dichloromethane solution (8 mL) of **6** (2.00 g, 4.69 mmol). After being allowed to warm to 25 °C, the mixture was stirred at 25 °C for 2 h and then evaporated to dryness under reduced pressure. Et_2O (2 mL) was added to the residue, and the resulting suspension was filtered through a glass filter. The filtrate was evaporated to dryness under reduced pressure. The residue was recrystallized from hexane to give $\mathbf{2_{tBu}}$ as a colorless crystalline material (1.48 g, 4.00 mmol) in 85% yield: FT-IR (ATR): ν (cm^{-1}) 3017, 2969, 2949, 2867, 1469, 1445, 1364, 1263, 1227, 1251, 1146, 1117, 1076, 1066, 877, 834, 809, 792, 756, 732, 696, 671, 658, 626, 596, 539, 527, 513, 497, 481, 465, 443, 437, 422. ^{1}H NMR (500 MHz, $CDCl_3$, 25 °C): δ (ppm) 8.46 (d, J = 2.6 Hz, 2H), 7.84 (dd, J = 8.8, 2.6 Hz, 2H), 7.54 (d, J = 8.8 Hz, 2H), 1.40 (s, 18H). ^{11}B NMR (160 MHz, $CDCl_3$, 25 °C): δ (ppm) 52.7 (br). ^{13}C NMR (125 MHz, $CDCl_3$, 25 °C): δ (ppm) 151.2, 150.5, 131.8, 129.8, 119.2, 34.7, 31.2, one peak of the carbon atoms (*ipso*-positions to the boron atom) were not observed. APCI-TOF mass: ion peaks assignable to the corresponding hydrolyzed product with a B–OH moiety were observed; calcd for $C_{20}H_{26}BO_2$ $[M+H]^+$: m/z=308.1946; found: 308.1910. ^{1}H and ^{13}C NMR spectra of $\mathbf{2_{tBu}}$ are shown in Figs. S23, S24 and S25, respectively.

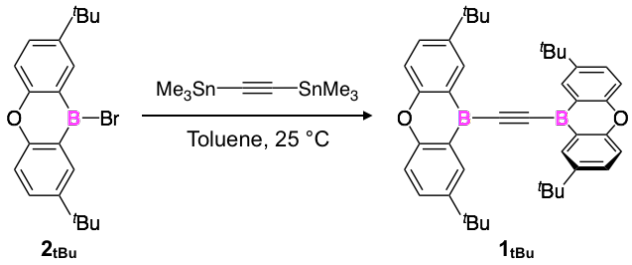

Compound $\mathbf{1_{tBu}}$. Under argon, a toluene solution (5.0 mL) of bis(trimethylstannyl)acetylene (0.90 g, 0.80 mmol) was added dropwise to a toluene solution (5.0 mL) of $\mathbf{2_{tBu}}$ (1.90 g, 1.89 mmol) at 25 °C, and the mixture was stirred at 25 °C for 1 h. The pale-yellow precipitate formed in the reaction mixture was collected by filtration, washed with hexane (5.0 mL x 3), and dried under reduced pressure to give $\mathbf{1_{tBu}}$ as a pale-yellow powder (144 mg, 0.23 mmol) in 28% yield: FT-IR (ATR): ν (cm^{-1}) 2959, 2866, 1603, 1577, 1552, 1481, 1455, 1415, 1362, 1339, 1305, 1276, 1258, 1228, 1142, 1130, 1112, 1051, 907, 827, 759, 683, 614, 587, 558, 524, 515, 509. ^{1}H NMR (500 MHz, $CDCl_3$, 25 °C): δ (ppm) 8.46 (d, J = 2.5 Hz, 2H), 7.85 (dd, J = 8.8, 2.5 Hz, 2H), 7.54 (d, J = 8.8 Hz, 2H), 1.14 (s, 18H). ^{11}B NMR (160 MHz,

$CDCl_3$, 25 °C): δ (ppm) 44.0 (br). ^{13}C NMR (125 MHz, $CDCl_3$, 25 °C): δ (ppm) 158.0, 144.9, 132.8, 131.7, 117.1, 34.5, 31.6, two peaks of the carbon atoms (*ipso*-positions to the boron atoms) were not observed. APCI-TOF mass: calcd for $C_{42}H_{48}O_2B_2$ $[M]^+$: m/z=606.3849; found: 606.3869. ^1H and ^{13}C NMR spectra of $\mathbf{1_{tBu}}$ are shown in Figs. S26, S27 and S28, respectively.

3. Single-crystal X-ray crystallography

A single crystal of $\mathbf{1_H}$, **3**, or **5**, which was obtained by recrystallization from CH_2Cl_2/hexane, toluene/hexane, or $CHCl_3$/hexane, respectively, was coated with an immersion oil (type B: Code 1248, Cargille Laboratories, Inc.) and mounted on a MicroMount (MiTeGen, LLC.). Diffraction data were collected at 90 K under a cold nitrogen gas stream on a RIGAKU model XtaLAB Synergy-DW diffractometer system equipped with a HyPix-6000 detector, using Cu-*K*α radiation (λ = 1.54184 Å).

Crystal data for $C_{26}H_{16}B_2O_2$ ($\mathbf{1_H}$): pale-yellow block, 0.20 x 0.20 x 0.15 mm^3, triclinic, $P\bar{1}$, a = 9.1910(4) Å, b = 9.2332(5) Å, c = 12.5455(7) Å, α = 70.147(5) °, β = 73.252(4) °, γ = 86.127(4) °, V = 958.35(9) $Å^3$, Z = 2, $density_{calcd}$ = 1.324 g cm^{-3}, T = 93 K, Cu-*K*α radiation, λ = 1.54184 Å, μ = 0.634 mm^{-1}, 7614 reflections measured, 3610 unique reflections, 271 parameters, R_{int} = 0.0143, Completeness to theta = 66.97°: 99.59%, Absorption correction: multi-scan, GOF = 1.053, $R1$ = 0.0358 ($I > 2\sigma(I)$), w$R2$ = 0.0970 (all data), $\Delta\rho_{min,\,max}$ = –0.172, 0.225 e$Å^3$, CCDC-2154677.

Crystal data for $C_{32}H_{16}B_2Co_2O_8$ (3): dark-green plate, 0.23 x 0.18 x 0.07 mm^3, triclinic, $P\bar{1}$, a = 9.2258(4) Å, b = 12.6088(4) Å, c = 12.6939(4) Å, α = 99.675(3) °, β = 108.556(4) °, γ = 102.399(3) °, V = 1417.43(9) $Å^3$, Z = 2, $density_{calcd}$ = 1.565 g cm^{-3}, T = 93 K, Cu-*K*α radiation, λ = 1.54184 Å, μ = 9.623 mm^{-1}, 16475 reflections measured, 5686 unique reflections, 398 parameters, R_{int} = 0.0764, Completeness to theta = 66.97°: 99.66%, Absorption correction: multi-scan, GOF = 1.033, $R1$ = 0.0696 ($I > 2\sigma(I)$), w$R2$ = 0.1959 (all data), $\Delta\rho_{min,\,max}$ = –0.625, 1.767 e$Å^3$, CCDC-2154678.

Crystal data for $C_{38}H_{24}B_3ClO_2$•$CHCl_3$ (5•$CHCl_3$): yellow block, 0.35 x 0.28 x 0.14 mm^3, monoclinic, $P2_1/c$, a = 17.1220(6) Å, b = 9.1966(4) Å, c = 21.6026(8), β = 108.556(4) °, V = 3224.8(2) $Å^3$, Z = 4, $density_{calcd}$ = 1.441 g cm^{-3}, T = 93 K, Cu-*K*α radiation, λ = 1.54184 Å, μ = 3.624 mm^{-1}, 20989 reflections measured, 6416 unique reflections, 434 parameters, R_{int} = 0.0475, Completeness to theta = 66.97°: 99.58%, Absorption correction: multi-scan, GOF = 1.130, $R1$ = 0.0568 ($I > 2\sigma(I)$), w$R2$ = 0.1745 (all data), $\Delta\rho_{min,\,max}$ = –0.857, 0.548 e$Å^3$, CCDC-2154679.

4. Device fabrication and characterization

Fabrication of OLED devices. A glass substrate coated with indium-tin oxide (ITO; 110 nm) was washed with acetone and isopropyl alcohol, and then exposed to UV/ozone for 10 minutes. An aqueous dispersion of poly(ethylenedioxy)thiophene:polystyrene sulfonic acid (PEDOT:PSS; 30 nm) was spin-coated on the ITO substrate, and the other layers were successively vacuum-deposited onto the resulting substrate with the following configuration; ITO (110 nm)/PEDOT:PSS (30nm)/tris(4-carbazoyl-9-ylphenyl)amine (TCTA) (20 nm)/6 wt% of an emitter and 94 wt% of a host (60 nm)/LiF (0.5 nm)/Al (100 nm). The current density-voltage characteristics and electroluminescence were recorded on a Keithley 2400 programmable source meter and a Konica Minolta model CS-2000 spectroradiometer.

Fabrication of hole-only devices (HODs). A glass substrate coated with ITO (110 nm) was washed with acetone and isopropyl alcohol, and then exposed to UV/ozone for 10 minutes. An aqueous dispersion of PEDOT:PSS (30 nm) was spin-coated on the ITO substrate, and the other layers were successively vacuum-deposited onto the resulting substrate with the following configuration; (110 nm)/PEDOT:PSS (30nm)/**1**$_{\mathbf{H}}$ or **1**$_{\mathbf{tBu}}$ (50 nm)/*N*,*N*'-di-1-naphthyl-*N*,*N*'-diphenyl benzidine (NPD) (30 nm)/Al (100 nm).

Fabrication of electron-only devices (EODs). A glass substrate coated with ITO (110 nm) was washed with acetone and isopropyl alcohol, and then exposed to UV/ozone for 10 minutes. The other layers were successively vacuum-deposited onto the resulting substrate with the following configuration; ITO/Ca (5 nm)/ **1**$_{\mathbf{H}}$ or **1**$_{\mathbf{tBu}}$ (50 nm)/LiF (0.5 nm)/Al (100 nm).

5. Theoretical calculations

Density functional theory (DFT) calculations were performed using the Gaussian 16 program package.[S3] The geometry optimization of **1**$_{\mathbf{H}}$ in the ground state in vacuum was performed using the B3LYP functional with a basis set of 6-31G(d). Cartesian coordinates and energy of the computed structure are listed in Tables S1.

Table S1. Optimized Cartesian coordinates of **1**$_{\mathbf{H}}$ (in Å) at the B3LYP/6-31G(d) level (–1200.255124 hartree).

O	-5.023500	-0.000300	-0.000100	C	3.213700	2.626500	2.651200
O	5.023500	0.000400	-0.000300	H	2.770400	3.324300	3.355700
C	2.957800	-0.913800	-0.922400	C	-4.363700	-0.851400	0.843300
C	2.957700	0.914000	0.922200	C	-4.363800	0.851100	-0.843400
C	-2.957800	0.922300	-0.914000	B	-2.134100	-0.000100	-0.000200
C	-2.957600	-0.922400	0.913800	C	-3.213700	-2.651000	2.626700
C	-3.214200	2.651200	-2.626500	H	-2.770300	-3.355300	3.324700
H	-2.771000	3.355700	-3.324400	B	2.134100	0.000100	-0.000100
C	4.363700	0.843600	0.851000	C	4.363800	-0.843200	-0.851300
C	3.214100	-2.626900	-2.650800	C	5.193200	1.638800	1.653800
H	2.770800	-3.324900	-3.355100	H	6.270300	1.544700	1.558800

C	2.410500	1.832100	1.849300	C	4.612300	2.525000	2.548700
H	1.328100	1.902500	1.920500	H	5.248500	3.145100	3.174700
C	-2.410800	1.849300	-1.832200	C	-4.612700	2.548600	-2.524800
H	-1.328400	1.920500	-1.902800	H	-5.249000	3.174600	-3.144900
C	-2.410400	-1.849200	1.832200	C	-4.612200	-2.548600	2.525200
H	-1.328000	-1.920300	1.902700	H	-5.248400	-3.174500	3.145400
C	-0.614200	0.000000	-0.000200	C	-5.193200	-1.654000	1.638700
C	2.410700	-1.832400	-1.849100	H	-6.270200	-1.559100	1.544600
H	1.328400	-1.903000	-1.920200	C	5.193400	-1.638600	-1.653800
C	0.614200	0.000000	-0.000200	H	6.270500	-1.544300	-1.558800
C	-5.193500	1.653800	-1.638500	C	4.612600	-2.525200	-2.548300
H	-6.270500	1.558700	-1.544300	H	5.248900	-3.145400	-3.174200

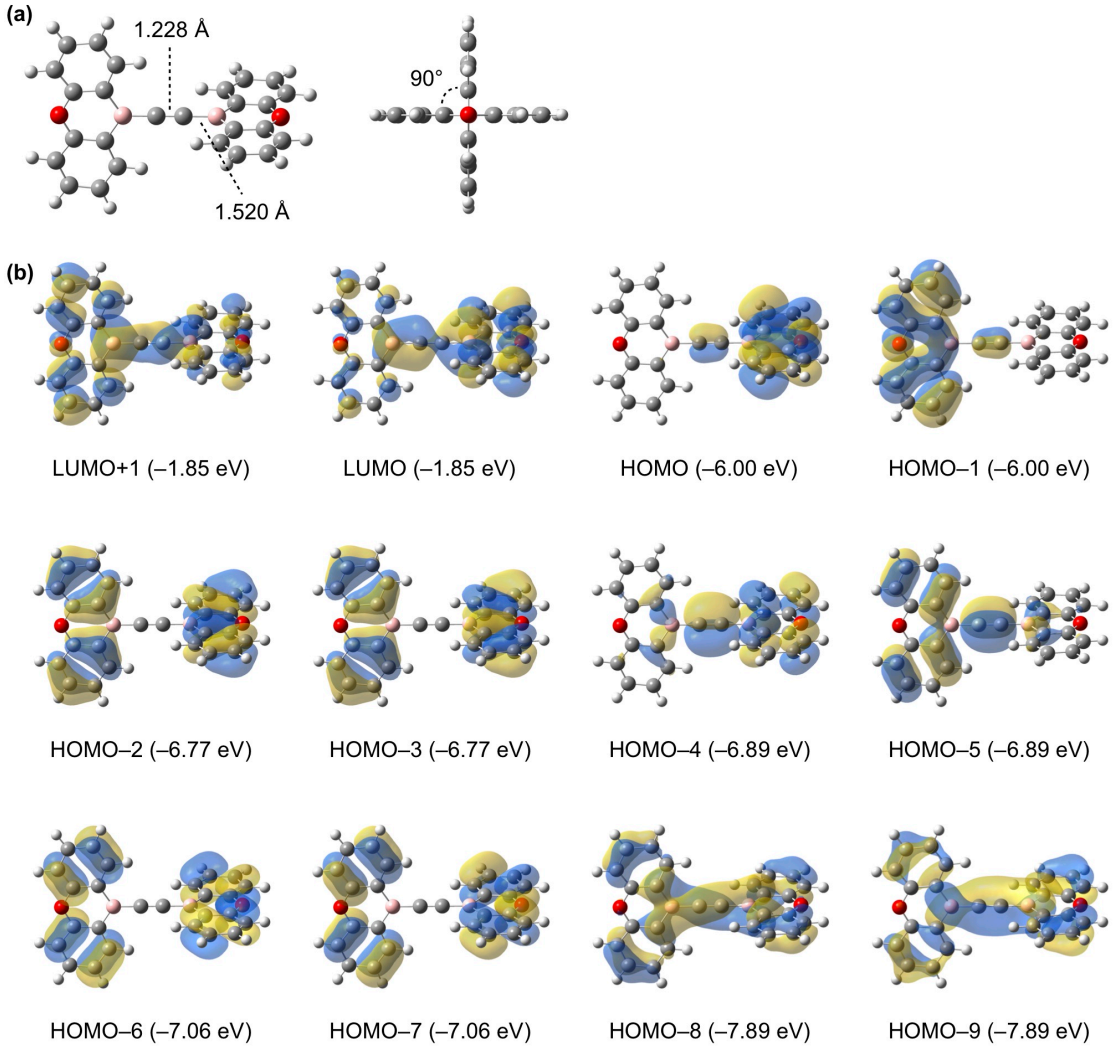

Figure S1. (a) Optimized geometry (left; top view and right; side view) and (b) its molecular orbitals and energies of $\mathbf{1_H}$ calculated at the B3LYP/6-31G(d) level.

6. Supporting References

S1. M. Melaïmi, S. Solé, C.-W. Chiu, H. Wang and F. P. Gabbaï, *Inorg. Chem.*, 2006, **45**, 8136−8143.

S2. A. R. White, L. Wang, D. A. Nicewicz, *Synlett*, 2019, **30**, 827–832.

S3. Gaussian 16, Revision C.01, M. J. Frisch, G. W. Trucks, H. B. Schlegel, G. E. Scuseria, M. A. Robb, J. R. Cheeseman, G. Scalmani, V. Barone, G. A. Petersson, H. Nakatsuji, X. Li, M. Caricato, A. V. Marenich, J. Bloino, B. G. Janesko, R. Gomperts, B. Mennucci, H. P. Hratchian, J. V. Ortiz, A. F. Izmaylov, J. L. Sonnenberg, D. Williams-Young, F. Ding, F. Lipparini, F. Egidi, J. Goings, B. Peng, A. Petrone, T. Henderson, D. Ranasinghe, V. G. Zakrzewski, J. Gao, N. Rega, G. Zheng, W. Liang, M. Hada, M. Ehara, K. Toyota, R. Fukuda, J. Hasegawa, M. Ishida, T. Nakajima, Y. Honda, O. Kitao, H. Nakai, T. Vreven, K. Throssell, J. A. Montgomery, Jr., J. E. Peralta, F. Ogliaro, M. J. Bearpark, J. J. Heyd, E. N. Brothers, K. N. Kudin, V. N. Staroverov, T. A. Keith, R. Kobayashi, J. Normand, K. Raghavachari, A. P. Rendell, J. C. Burant, S. S. Iyengar, J. Tomasi, M. Cossi, J. M. Millam, M. Klene, C. Adamo, R. Cammi, J. W. Ochterski, R. L. Martin, K. Morokuma, O. Farkas, J. B. Foresman, and D. J. Fox, Gaussian, Inc., Wallingford CT, **2016**.

S4. M. Singh, D. k. Dubey and J. Jou, 2017 IEEE 3rd International Future Energy Electronics Conference and ECCE Asia (IFEEC 2017–ECCE Asia), 2017, 1043, doi: 10.1109/IFEEC.2017.7992185.

7. Supporting Figures

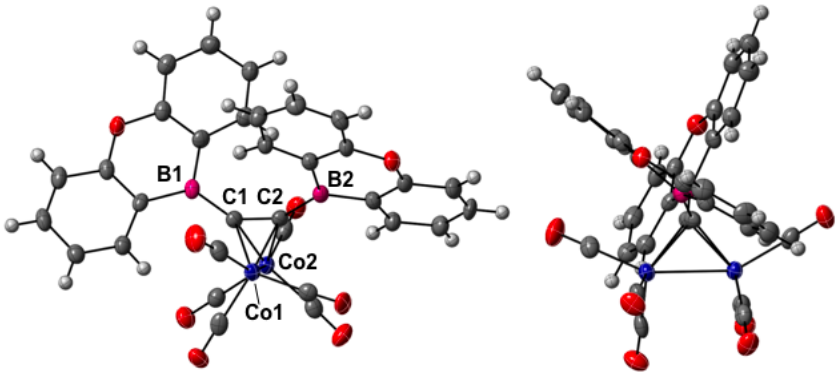

Figure S2. X-ray crystal structure of **3** (left; top view and right; side view) with atomic displacement parameters set at 50% probability. Color code: hydrogen = white, boron = pink, carbon = gray, oxygen = red and cobalt = blue. Selected bond lengths (Å) and angles (°): C(1)–C(2) = 1.334(6), C(1)–B(1) = 1.537(7), C(1)–Co(1) = 1.998(5), C(1)–Co(2) = 2.022(4), C(2)–B(2) = 1.546(6), C(2)–Co(1) = 2.001(4), C(2)–Co(2) = 2.002(4), B(1)–C(1)–C(2) = 143.5(4), C(1)–C(2)–B(2) = 147.0(4), B(1)–C(1)–C(2)–B(2) = –47.7(11).

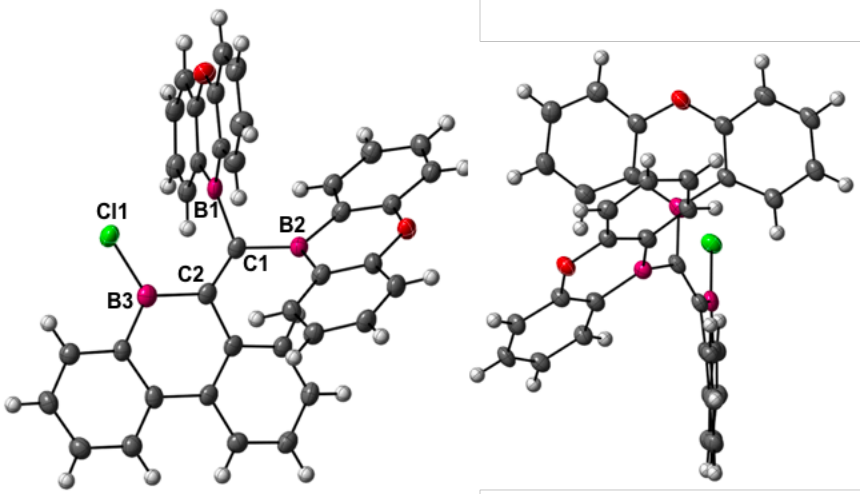

Figure S3. X-ray crystal structure of **5** (left; top view and right; side view) with atomic displacement parameters set at 50% probability. Color code: hydrogen = white, boron = pink, carbon = gray, oxygen = red and chlorine = green. Selected bond lengths (Å) and angles (°): C(1)–C(2) = 1.371(4), C(1)–B(1) = 1.581(4), C(1)–B(2) = 1.588(4), C(2)–B(3) = 1.544(4), C(2)–C(38) = 1.480(4), B(3)–Cl(1) = 1.771(3), B(1)–C(1)–C(2)–B(3) = 27.1(4), B(1)–C(1)–C(2)–C(38) = –165.3(3), B(2)–C(1)–C(2)–C(38) = 16.2(4), B(2)–C(1)–C(2)–B(3) = –150.4(3).

.

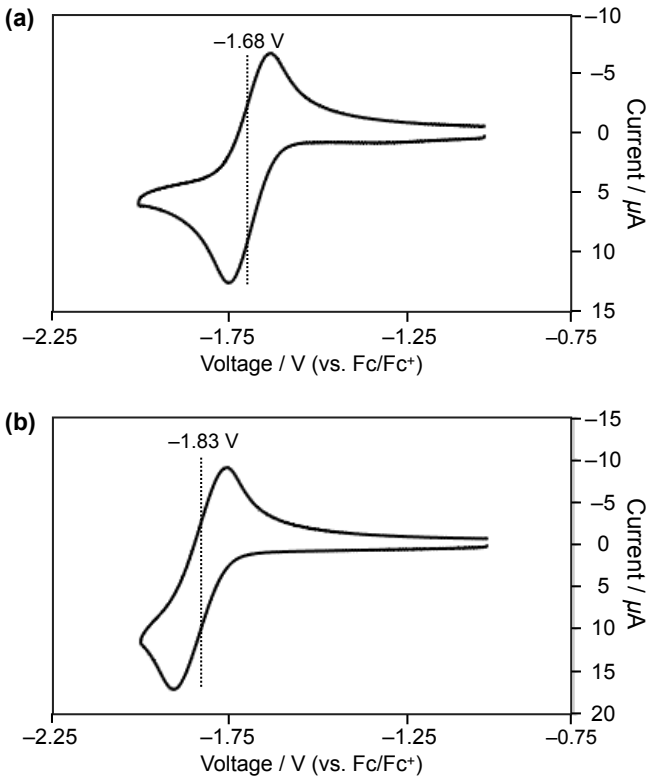

Figure S4. Cyclic voltammograms of (a) $\mathbf{1_H}$ (1.0×10^{-4} M) and (b) $\mathbf{1_{tBu}}$ (1.0×10^{-4} M) in THF containing tetrabutylammonium hexafluorophosphate (0.1 M) as a supporting electrolyte at a scan rate of 100 mV s^{-1}.

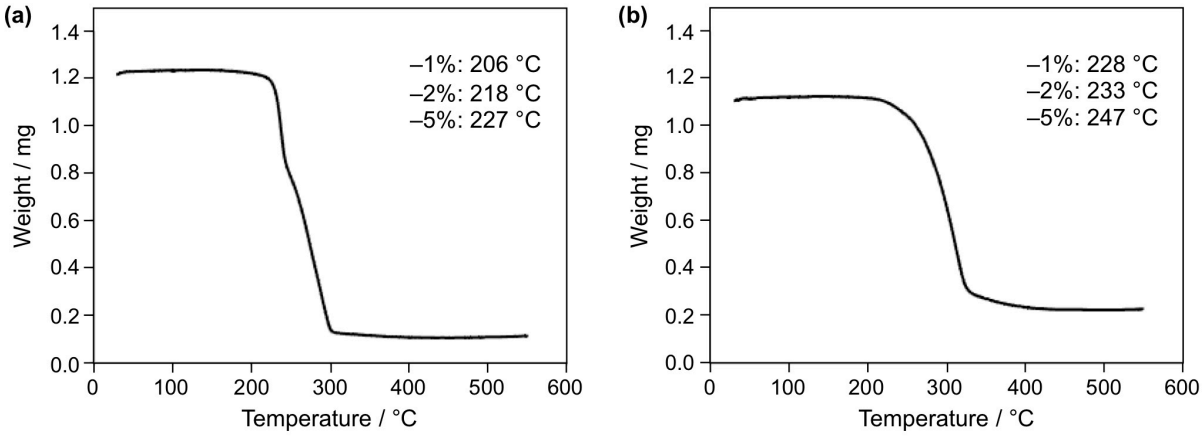

Figure S5. TGA profiles of (a) $\mathbf{1_H}$ and (b) $\mathbf{1_{tBu}}$ under N_2 measured at a heating rate of 10 °C/min.

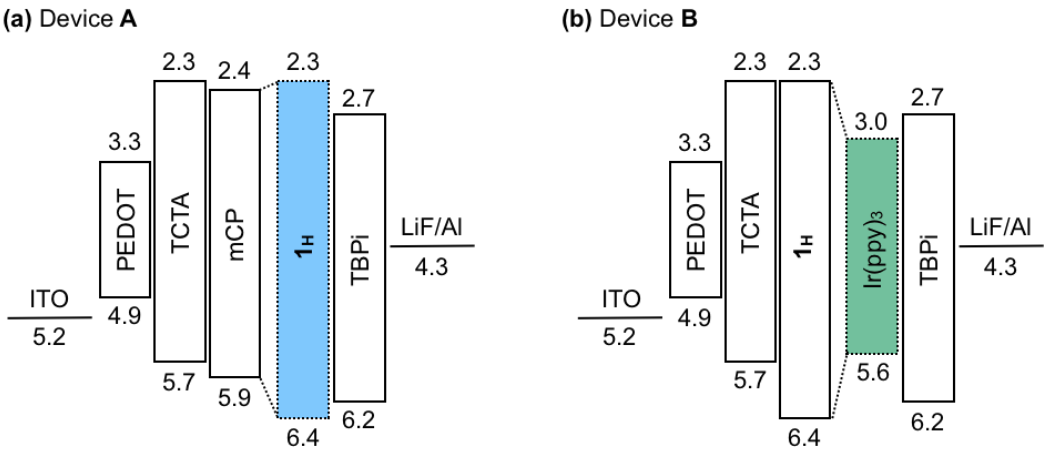

Figure S6. Energy-level diagrams for OLED devices **A** and **B** (in eV). The HOMO level and HOMO-LUMO gap of $\mathbf{1_H}$ were estimated based on photoelectron spectroscopy and DFT calculations, respectively. The energy levels of other layers were taken from ref. S4.

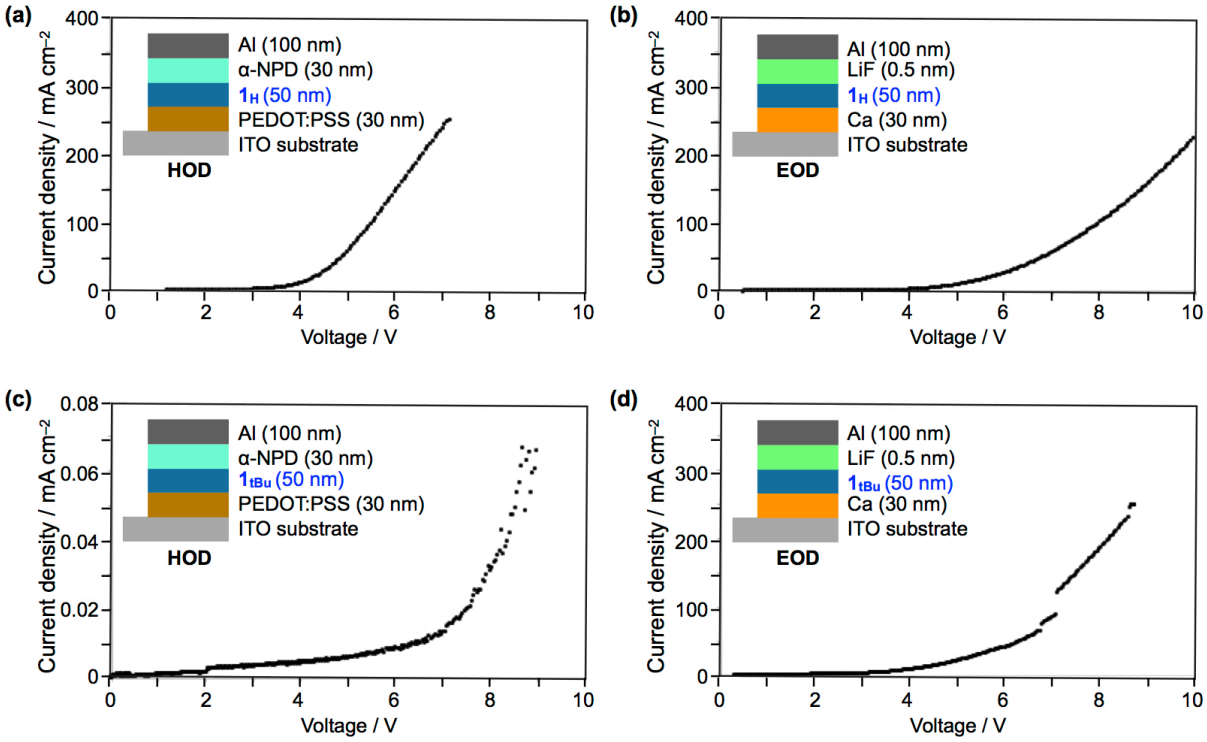

Figure S7. *J–V* characteristics of (a) a hole-only device (HOD) and (b) an electron-only device (EOD) with a layer of $\mathbf{1_H}$ (inset: device configurations). Charge-carrier mobilities for the HOD and EOD, evaluated based on a space-charge-limited current (SCLC) technique, were determined to be 2.9 x 10^{-6} and 2.1 x 10^{-6} cm^2 V^{-1} s^{-1}, respectively. *J–V* characteristics of (c) a HOD and (d) an EOD with a layer of $\mathbf{1_{tBu}}$ (inset: device configurations). Charge-carrier mobilities for the HOD and EOD, evaluated based on a SCLC technique, were determined to be 3.6 x 10^{-10} and 6.0 x 10^{-6} cm^2 V^{-1} s^{-1}, respectively.

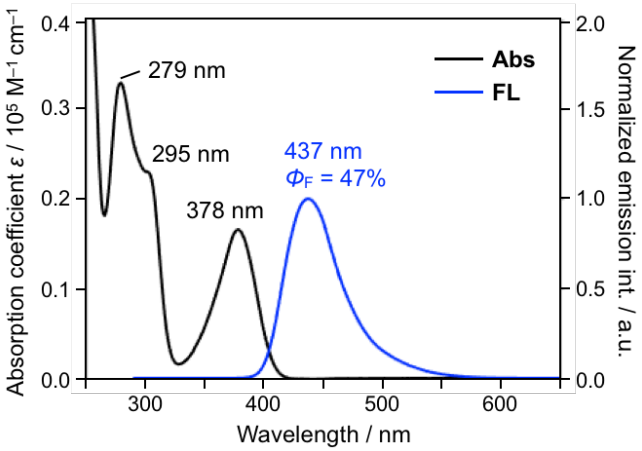

Figure S8. Electronic absorption (black) and fluorescence (blue, λ_{ex} = 279 nm) spectra of $\mathbf{1_H}$ in CH_2Cl_2 (1.0×10^{-5} M) at 25 °C.

8. Analytical data

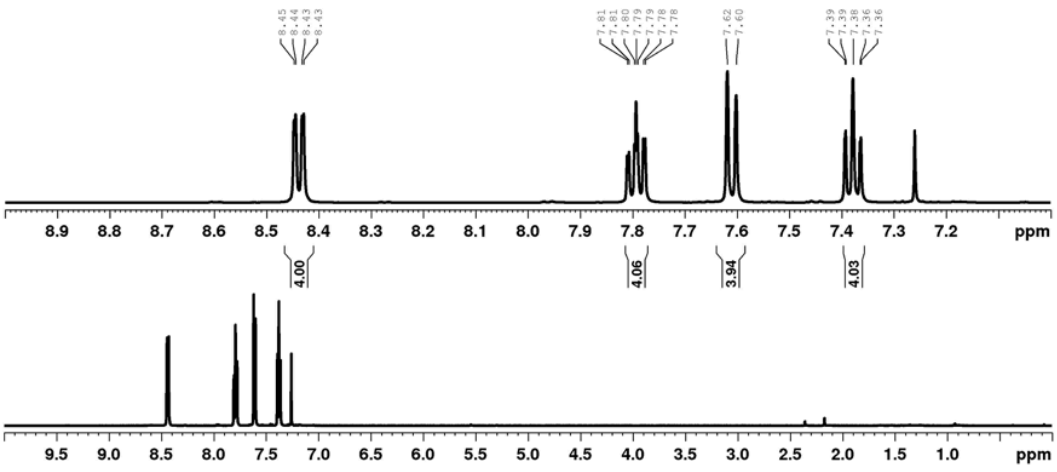

Figure S9. ^{1}H NMR spectrum (500 MHz) of $\mathbf{1_H}$ in $CDCl_3$ at 25 °C and its magnified view.

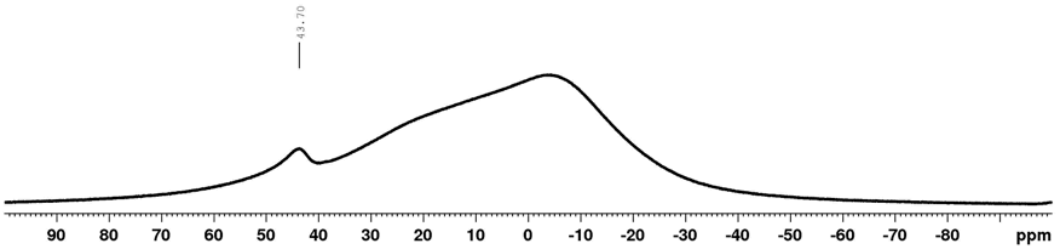

Figure S10. ^{11}B NMR spectrum (160 MHz) of $\mathbf{1_H}$ in $CDCl_3$ at 25 °C. The broad peaks in a region from 50 to –40 ppm are the contribution from a borosilicate-glass NMR tube.

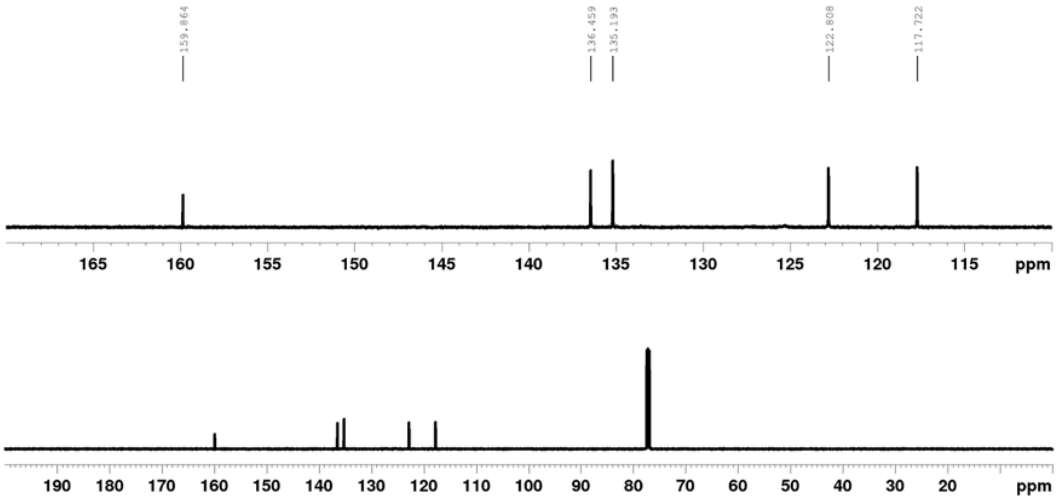

Figure S11. ^{13}C NMR spectrum (125 MHz) of $\mathbf{1_H}$ in $CDCl_3$ at 25 °C and its magnified view.

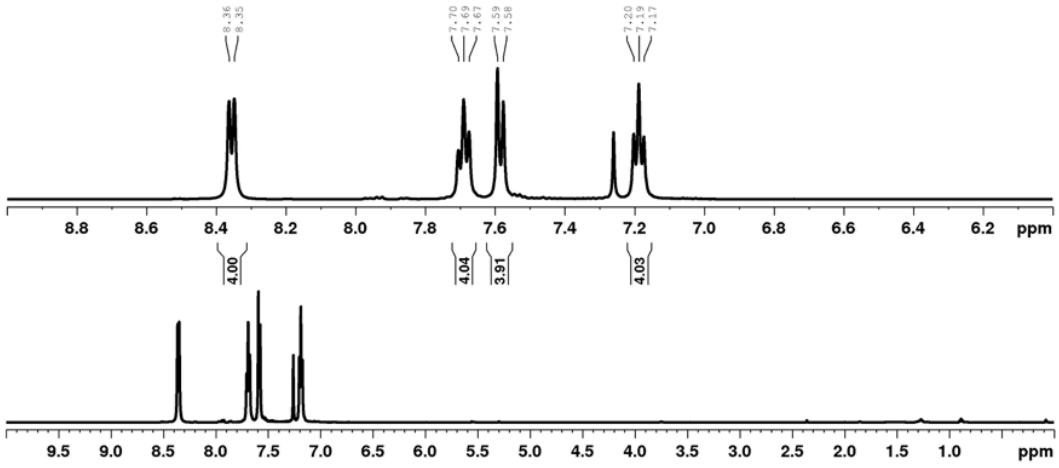

Figure S12. ^{1}H NMR spectrum (500 MHz) of **3** in $CDCl_3$ at 25 °C and its magnified view.

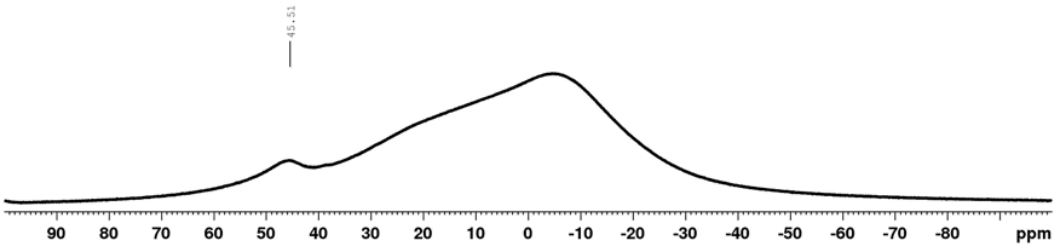

Figure S13. ^{11}B NMR spectrum (160 MHz) of **3** in $CDCl_3$ at 25 °C. The broad peaks in a region from 50 to –40 ppm are the contribution from a borosilicate-glass NMR tube.

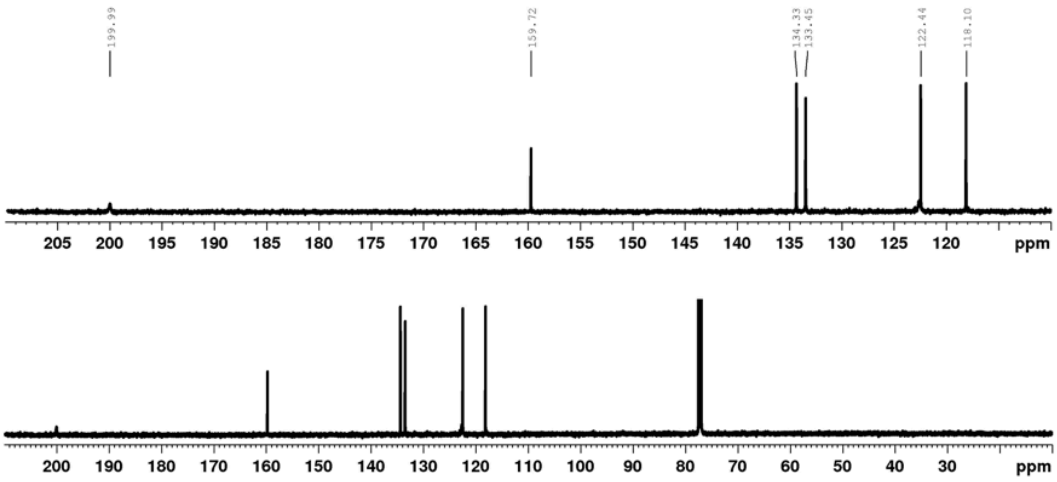

Figure S14. ^{13}C NMR spectrum (125 MHz) of **3** in $CDCl_3$ at 25 °C and its magnified view.

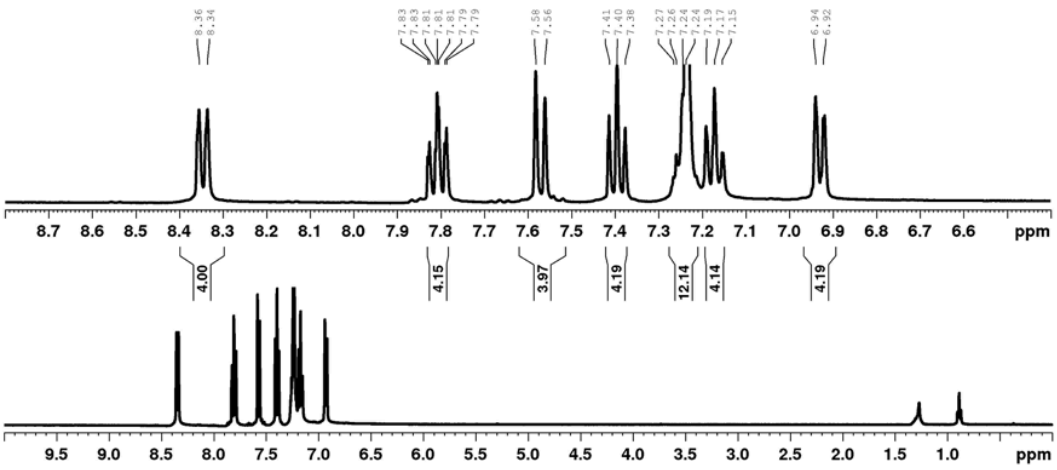

Figure S15. ^{1}H NMR spectrum (500 MHz) of **4** in $CDCl_3$ at 25 °C and its magnified view.

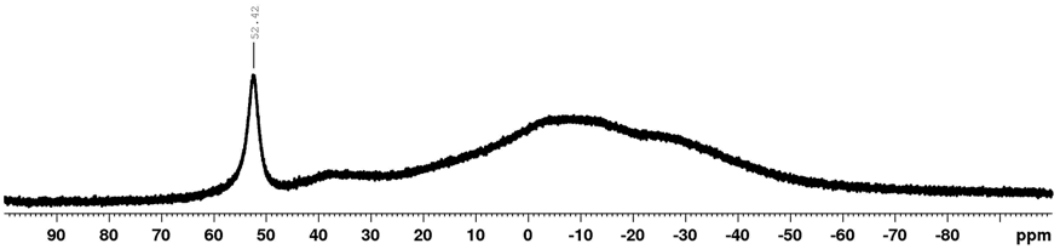

Figure S16. ^{11}B NMR spectrum (160 MHz) of **4** in $CDCl_3$ at 25 °C. The broad peaks in a region from 50 to –40 ppm are the contribution from a borosilicate-glass NMR tube.

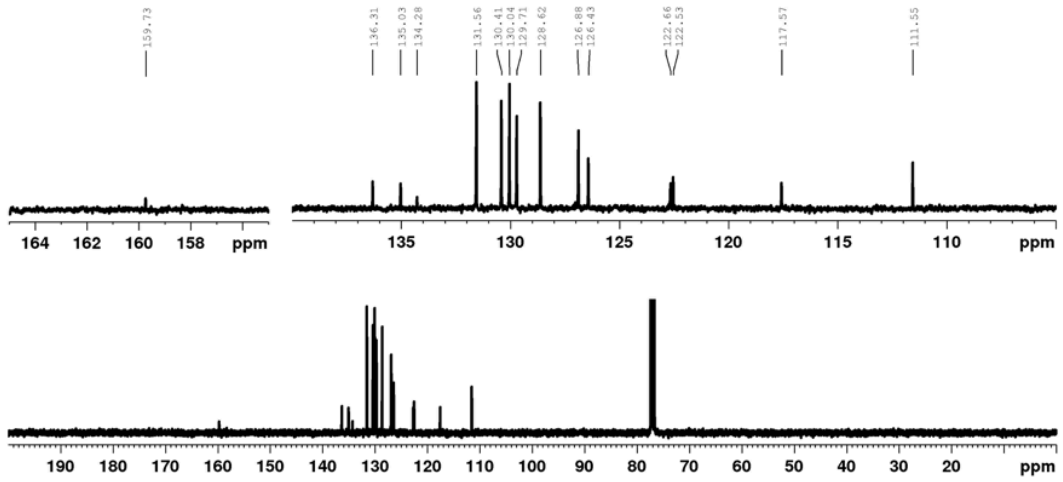

Figure S17. ^{13}C NMR spectrum (125 MHz) of **4** in $CDCl_3$ at 25 °C and its magnified view.

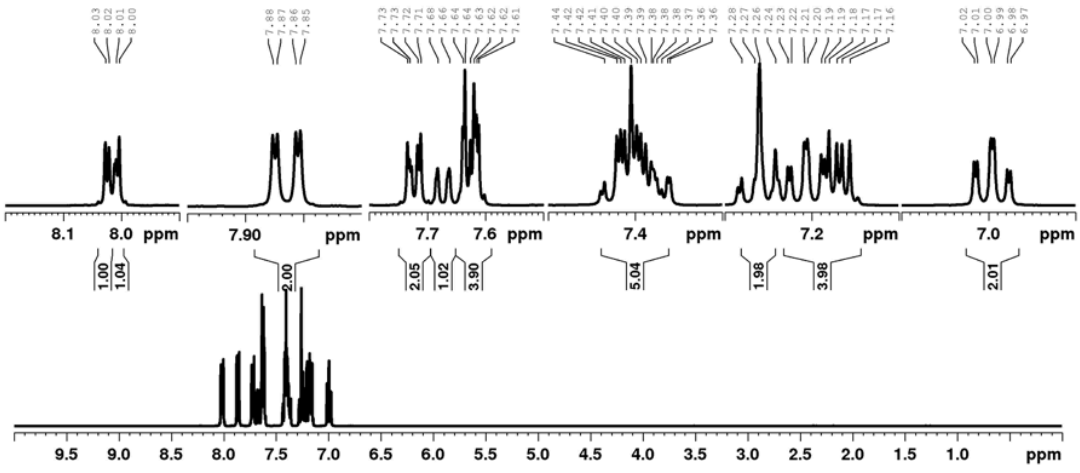

Figure S18. ^{1}H NMR spectrum (500 MHz) of **5** in $CDCl_3$ at 25 °C and its magnified view.

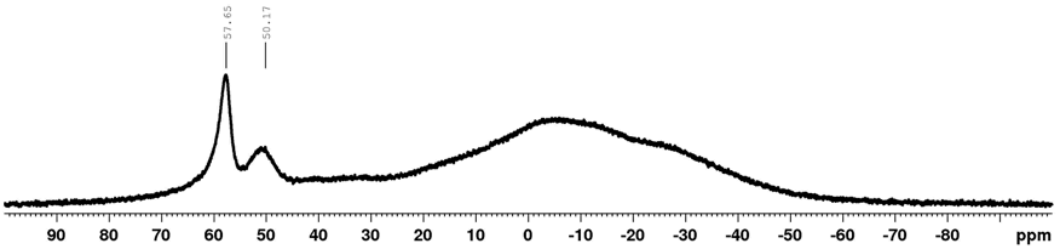

Figure S19. ^{11}B NMR spectrum (160 MHz) of **5** in $CDCl_3$ at 25 °C. The broad peaks in a region from 50 to –40 ppm are the contribution from a borosilicate-glass NMR tube.

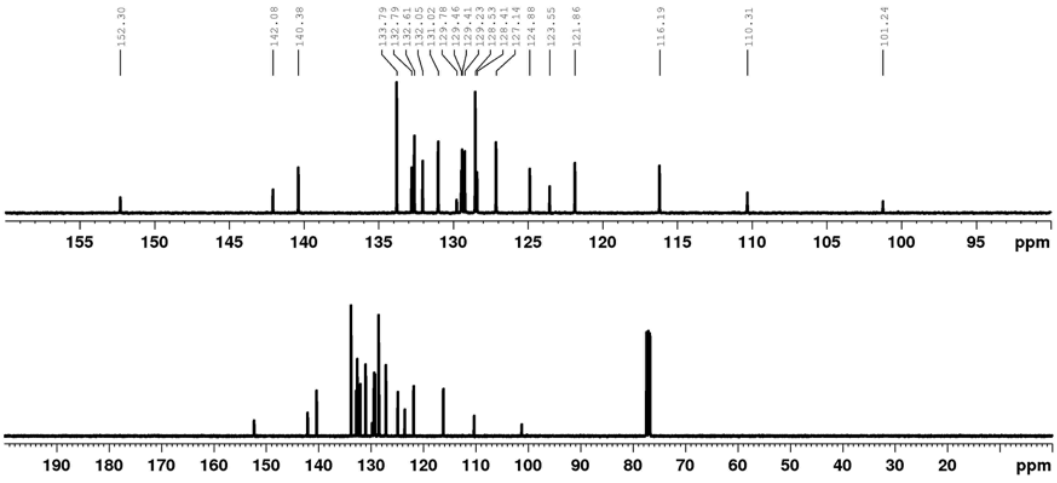

Figure S20. ^{13}C NMR spectrum (125 MHz) of **5** in $CDCl_3$ at 25 °C and its magnified view.

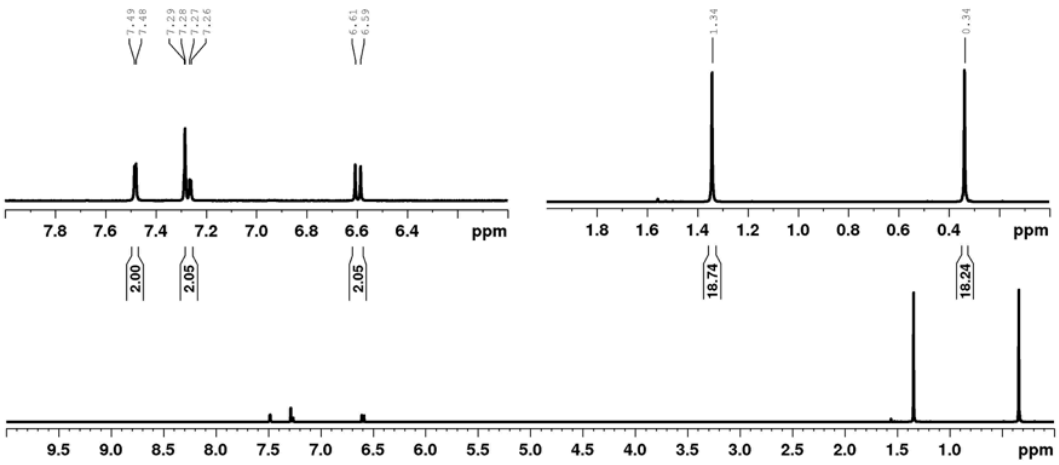

Figure S21. ^{1}H NMR spectrum (500 MHz) of **6** in $CDCl_3$ at 25 °C and its magnified view.

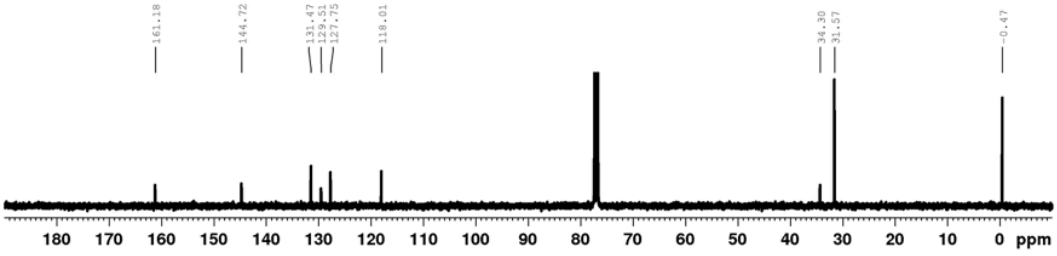

Figure S22. ^{13}C NMR spectrum (125 MHz) of **6** in $CDCl_3$ at 25 °C.

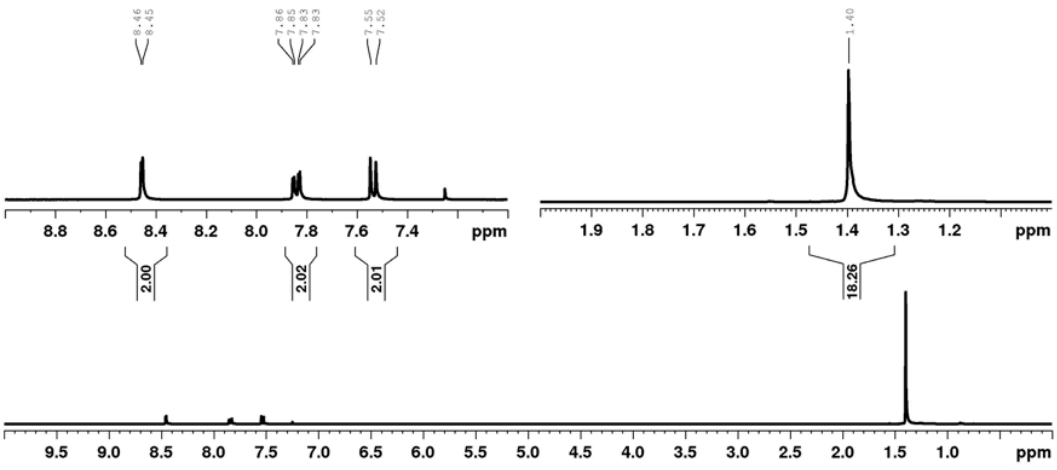

Figure S23. ^{1}H NMR spectrum (500 MHz) of $\mathbf{2_{tBu}}$ in $CDCl_3$ at 25 °C and its magnified view.

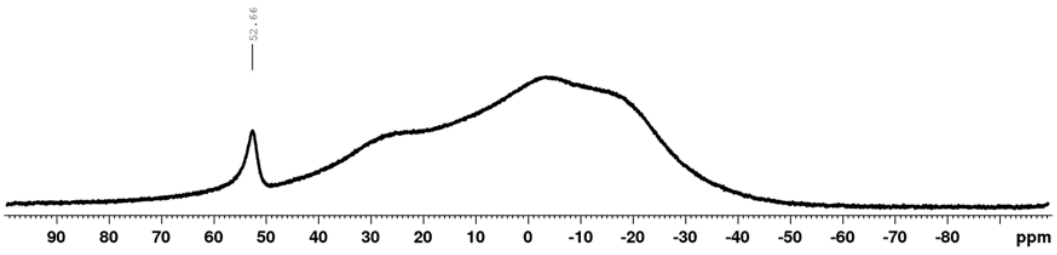

Figure S24. ^{11}B NMR spectrum (160 MHz) of $\mathbf{2_{tBu}}$ in $CDCl_3$ at 25 °C. The broad peaks in a region from 50 to –40 ppm are the contribution from a borosilicate-glass NMR tube.

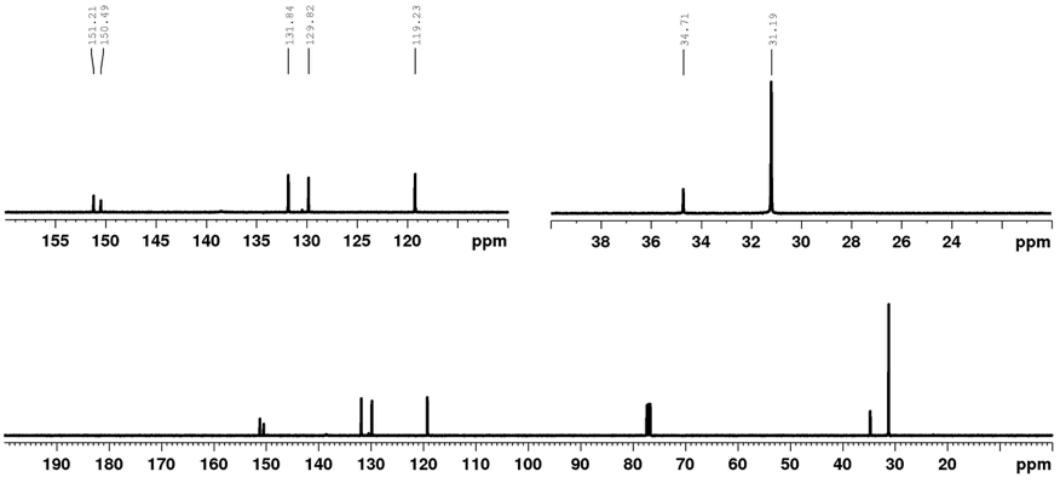

Figure S25. ^{13}C NMR spectrum (125 MHz) of $\mathbf{2_{tBu}}$ in $CDCl_3$ at 25 °C and its magnified view.

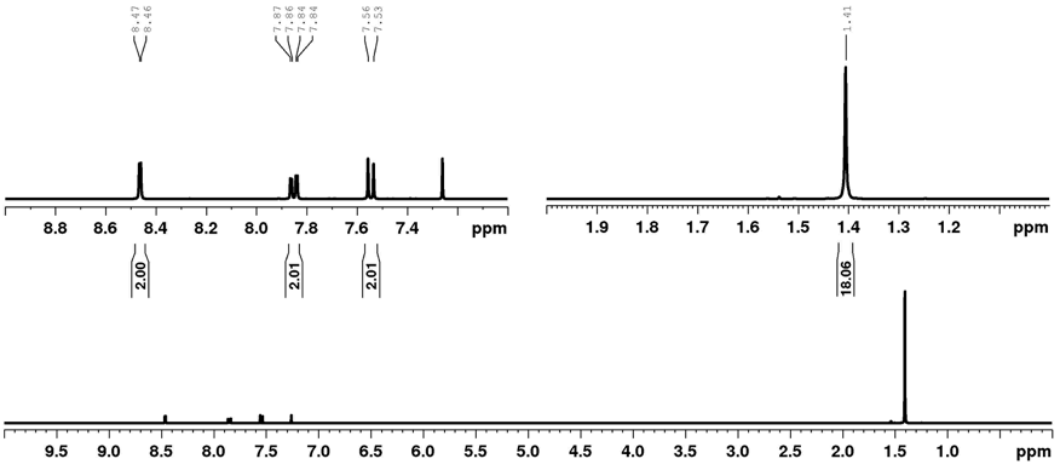

Figure S26. ^{1}H NMR spectrum (500 MHz) of $\mathbf{1_{tBu}}$ in $CDCl_3$ at 25 °C and its magnified view.

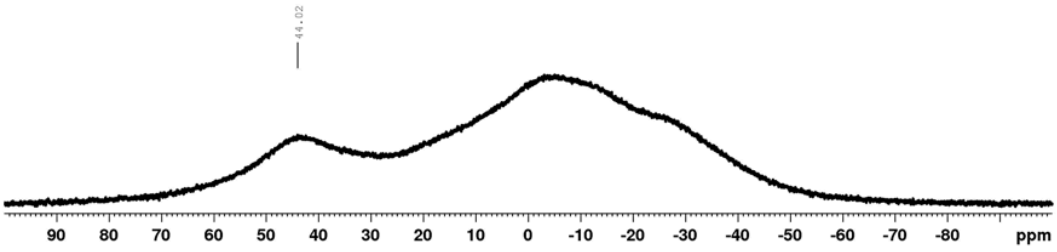

Figure S27. ^{11}B NMR spectrum (160 MHz) of $\mathbf{1_{tBu}}$ in $CDCl_3$ at 25 °C. The broad peaks in a region from 50 to –40 ppm are the contribution from a borosilicate-glass NMR tube.

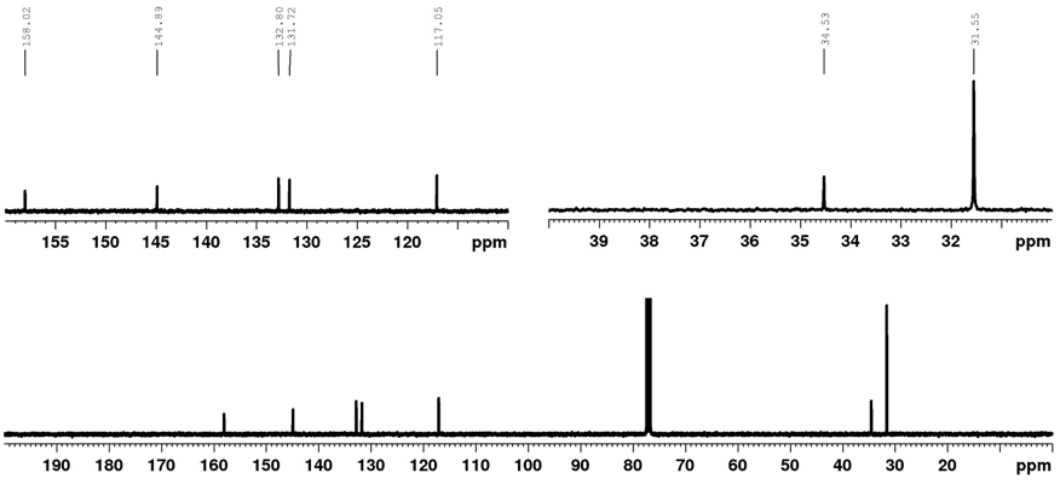

Figure S28. ^{13}C NMR spectrum (125 MHz) of $\mathbf{1_{tBu}}$ in $CDCl_3$ at 25 °C and its magnified view.